



# Comparison of Different Leaching Media and Their Effect on REEs Recovery from Spent Nd-Fe-B Magnets

FUPENG LIU <sup>1,2</sup> ANTTI PORVALI,<sup>2</sup> PETTERI HALLI,<sup>2</sup>  
BENJAMIN P. WILSON,<sup>2</sup> and MARI LUNDSTRÖM<sup>2,3</sup>

1.—Institute of Engineering Research, Jiangxi University of Science and Technology, Ganzhou 341000, China. 2.—Hydrometallurgy and Corrosion, Department of Chemical and Metallurgical Engineering (CMET), School of Chemical Engineering, Aalto University, P.O. Box 12200, 00076 Espoo, Finland. 3.—e-mail: mari.lundstrom@aalto.fi

Recycling rare-earth elements (REEs) from Nd-Fe-B magnet waste is an important step towards building a sustainable REE supply chain. In this study, two different processes were systematically investigated and compared. In the leaching stage, the effect of increasing H<sub>2</sub>SO<sub>4</sub> or HCl concentrations were studied and it was determined that, although both can successfully promote REEs, B, Fe and Co leaching, HCl solutions extracted a wider range of metals. After leaching, the oxalate and double-sulfate precipitation methods were utilized to separate REEs from either HCl or H<sub>2</sub>SO<sub>4</sub> leachates. Results suggest that, although > 99% REEs precipitation rates could be achieved with oxalate, the purity of REE-containing products is significantly affected by impurities like Fe and Co. In contrast, REE double-sulfate precipitation resulted in a product purity of > 99%; however, high levels of Na<sub>2</sub>SO<sub>4</sub> (8 times the stoichiometric amount) were needed to achieve > 98% of REE precipitation.

## INTRODUCTION

Neodymium–iron–boron (Nd-Fe-B) permanent magnets are the strongest permanent magnetic materials known and are utilized in everyday life in a variety of essential high-tech applications, like the electrical motors found in, e.g., cars, elevators and wind power generators.<sup>1</sup> Nevertheless, these magnets contain a large quantity of rare earth elements (REEs) such as neodymium (Nd), classified as critical raw material by the European Union, and smaller quantities of praseodymium (Pr) and dysprosium (Dy).<sup>2</sup>

REEs are found in a number of different minerals like monazite, xenotime and bastnaesite, and are relatively common elements within the Earth's crust.<sup>3</sup> In fact, a majority of REEs are not exceptionally scarce; for example, cerium, neodymium (Nd), lanthanum (La) and yttrium (Yt) are more abundant than lead (Pb), and generally all REEs, with the exception of radioactive promethium (Pm), are more available than cadmium (Cd) in the asthenosphere.<sup>4</sup> Despite this relative abundance, REEs are often only found in dilute concentrations

in ores, make them costly and difficult to process chemically. Nonetheless, several secondary waste streams like those related to NiMH batteries and Nd-Fe-B permanent magnets are rich in REEs.<sup>3</sup> However, until recently a majority of the REEs in such wastes have been lost into different unrecoverable fractions.<sup>5</sup> Consequently, it is evident that current industrial processes treating permanent magnet waste need to be improved in order to ensure the more sustainable use of scarce valuable metals, like REEs, that have a limited availability.

Current Nd-Fe-B magnet recycling methods often make use of sulfuric acid and hydrochloric acid as the lixiviant.<sup>6</sup> Additionally, in order to avoid the generation of toxic gases and achieve the concurrent selective separation of REEs from the waste material, processing is often preceded by an oxidative roasting treatment that forms solid phases such as Fe<sub>2</sub>O<sub>3</sub> and REE<sub>2</sub>O<sub>3</sub> which have a different reactivity towards the selected lixiviant.<sup>7</sup> Other aspects, like the effect of particle size (< 80 μm and < 400 μm) on the oxidation of REEs and Fe in spent Nd-Fe-B magnets have been studied; however, due to an absence of particle size distribution data, it is not

possible to draw any conclusions related to the influence of dominative particle size.<sup>8</sup> In the present study, the effect of particle size classes during the roasting step was studied, as diffusion has previously been found to be a limiting factor in oxidation.<sup>9</sup> Experiments on well-defined particle size classes with TGA (thermo-gravimetric analysis) revealed that diffusion limitations have practical constraints on the maximum particle size that can be oxidized within a reasonable timeframe. Through optimization of the oxidation–roasting process, it is possible to avoid both unnecessary energy consumption and the formation of insoluble phases like REE-ferrate.

The roasting experiments were followed by comparative leaching experiments. As Nd-Fe-B magnets are primarily composed of Fe (> 50 wt.%),<sup>6</sup> it is imperative that Fe dissolution is avoided in order to reduce the reagent consumption and valueless waste generation. Hematite and REE<sub>2</sub>O<sub>3</sub> have significantly different dissolution pH ranges, and this fact has previously been exploited for the selective recovery of REEs.<sup>10</sup> There have been several studies<sup>6–10</sup> where selective leaching of Nd-Fe-B magnets after oxidative roasting has been investigated; however, these studies often fail to explore the effects of oxidative roasting on the REEs recovery from spent magnets. In addition, the effects of different lixiviants (e.g., HCl and H<sub>2</sub>SO<sub>4</sub>) on the leaching kinetics of the main metals (REEs, B, Co and Fe) have also rarely been reported in the open literature.

After leaching, REEs are typically recovered either as oxalates (from HCl leachate) or double-sulfates (H<sub>2</sub>SO<sub>4</sub> leachate), although there are a few studies about the effects of these different leaching media on the subsequent REEs recovery processes. In the case of double-sulfates, the challenges may relate to the precipitation of the heavier REEs, like Dy and Gd, as their solubility is significantly higher than that of lighter REEs, such as Pr and Nd.<sup>11</sup> As a result of these contrasting solubilities, different recovery strategies for heavy and light REEs in sulfate media could be required. Conversely, even though REE-oxalates tend to be insoluble,<sup>12</sup> oxalate ions may also complex strongly with dissolved iron,<sup>13</sup> causing inefficient precipitant utilization and low-purity REEs products. As a consequence, the selection of REE precipitation methods should be investigated from the perspective of recovery efficiencies, costs and final product purity.

Based on the current status of Nd-Fe-B recovery methods, a systematic study of oxidative roasting was initially carried out. This was then followed by in-depth investigations into the leaching kinetics of valuable metals with two different acid leaching systems, H<sub>2</sub>SO<sub>4</sub> and HCl, and their effect on the purity of the subsequent products was compared. These results provide more informative data related to process selection and enhancement for industrial Nd-Fe-B recycling.

## EXPERIMENTAL

### Pretreatment and Characterization

The spent Nd-Fe-B magnets, originally manufactured by sintering, were cleaned prior to demagnetization at 500°C for 2 h under atmospheric air, before being sequentially comminuted by a jaw crusher (MN 931; Wedage, Germany) and then a ring mill (Pulverisette 9; Fritsch, Germany). After 60–75 s of ring milling, the particles were processed by a sieving machine (AS 30; Retsch, Germany) with fraction intervals of 25 μm, 63 μm, 180 μm, 355 μm, and 450 μm, and separate samples were taken from each particle size class. The overflow was then remilled for a further 60 s in order to achieve a particle size of less than 200 μm for the whole sample. The fine powder obtained was then subjected to particle size distribution (PSD) determination by laser diffraction (Mastersizer 3000; Malvern, UK) using an input feed air pressure of 3–4 bar and the results were analyzed using a Fraunhofer diffraction model.

After mechanical pre-treatment, the raw material was chemically characterized by ICP-OES (inductively coupled plasma–optical emission spectroscopy; Optima DV7100; Perkin Elmer, USA) with all the primary elements commonly found within Nd-Fe-B magnets analyzed, including Fe, Nd, Dy, Pr, Gd, Co and B.

### Roasting

Roasting experiments were performed in two different furnaces, and, in all cases, the degree of oxidation was determined based on mass change, with samples being weighed before and after the experiments. In addition, TGA was performed under temperature control with a vertical furnace (THV12/80/610-2408CP; Elite Thermal Systems, UK) (see supplementary Fig. S-1). Samples of 1 g were evenly distributed within an Al<sub>2</sub>O<sub>3</sub> crucible to a depth of ca. 1 cm, before being placed in the furnace hot zone with aluchrome S wire. The temperature difference within the hot zone was determined to be ± 2°C and was measured with a calibrated S-type thermocouple (Pt/90% Pt–10% Rh; Johnson-Matthey, UK), connected to an automated logging set-up (Data logger; Keithley, USA) combined with LabVIEW (National Instruments, USA). Changes in sample weight during roasting were measured in situ using an analytical balance (AB204-S; Mettler-Toledo, USA) and airflow speed was calculated based on the lift experienced by the crucible inside the furnace. In total, four different temperatures were investigated: 500°C, 600°C, 700°C, and 800°C, and additional experiments using the different particle size samples were performed at 800°C. The main mineral phases within the samples before and after roasting were identified by x-ray diffraction (XRD; PANalytical X'Pert Pro Powder; Almelo, Netherlands) using a CoK $\alpha$

radiation source with a 40-kV acceleration potential and current of 40 mA, and the resultant XRD diffractograms were analyzed using HighScore 4.0 Plus software.

Based on the results of the TGA experiments, temperatures of 700°C and 800°C were selected for further investigation using a previously described horizontal furnace set-up.<sup>14</sup> Within the furnace, the flow of oxidant—technical air (20.9 vol.% O<sub>2</sub>, 79.1 vol.% N<sub>2</sub>; AGA, Finland)—was carefully controlled and different flow rates and durations were applied (see supplementary Table S-I). Samples were inserted into the cold furnace within an Al<sub>2</sub>O<sub>3</sub> crucible and heated at 200°C/h under a protective argon (99.999 vol.%) atmosphere to the desired target temperature, after which the gas feed was instantaneously switched from argon to air to initiate the experiment. Once the required experimental duration was achieved, the atmosphere was changed back to argon and the furnace was cooled at 200°C/h. After the roasting was complete and the crucible sufficiently cool, the samples were weighed.

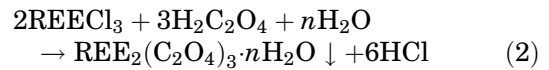
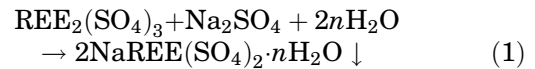
## Leaching

The leaching experiments were performed in a 300-mL cylindrical reactor with mechanical stirring (300 rpm), and the temperature (80°C) was controlled by a water bath (DC10, Thermo Haake®; USA). Prior to each run, 200 mL of either sulfuric or hydrochloric acid solution was placed in the reactor vessel and then heated to a preset temperature, before the addition of the previously roasted spent Nd-Fe-B magnets to a known initial liquid to solid ratio (*L/S*, mL/g). After a predetermined experimental time, the resultant slurry was filtered to obtain a cake and a filtrate. The filter cake was subsequently rinsed with deionized water to obtain the leach residue, and the volume of the leachate and wash water were accurately recorded. Solution concentrations of REEs, Fe, Co and B were measured using ICP-OES. The extraction of REEs, Fe, Co and B was determined as a function of leaching time (10–240 min) and acid concentration (0.5–4 mol/L) at an *L/S* of 10.

## REEs Precipitation

In the sulfuric acid leaching system, the alkali double-sulfate precipitation method was carried out to recover the REEs. In contrast, the oxalate precipitation method was used to recover the REEs in the hydrochloric acid leaching system. These precipitation experiments were performed by adding 100 mL of the resulting leachate into a 250-mL conical flask, which was then heated to either 70°C (double-salt precipitation) or 50°C (oxalate precipitation) for 1 h with magnetic stirring (200 rpm) and precipitants, Na<sub>2</sub>SO<sub>4</sub> or H<sub>2</sub>C<sub>2</sub>O<sub>4</sub>, were added to the solution in order to recover the REEs. After a known time interval, the resultant precipitate was filtered, washed with distilled water, and then dried at

100°C for 12 h. The volume of the leachate and wash water were also recorded. The theoretical amounts of sodium sulfate and oxalic acid required for precipitation were deduced from Eqs. 1 and 2:



The precipitation of REEs (%*P*) was calculated as follows:

$$\%P = [(1 - (V_1 \times C_1 + V_2 \times C_2) / (V_0 \times C_0))] \times 100\% \quad (3)$$

where *C*<sub>0</sub> and *C*<sub>1</sub> represent the initial and final concentration of REEs before and after the precipitation procedure, *V*<sub>0</sub> and *V*<sub>1</sub>, the volume of solution before and after precipitation, *C*<sub>2</sub> represents the concentration of REEs in washing water, and *V*<sub>2</sub> the volume of associated washing water.

## RESULTS AND DISCUSSION

### Pre-treatment and Roasting

TGA analyses were initially performed on the different particle size classes at 800°C, with the selected temperature chosen based on literature; at this temperature, it is possible to obtain the desired oxides at a higher rate, as demonstrated by the extensive thermal oxidation investigation of Nd-Fe-B particles performed previously by Firdaus et al.<sup>7</sup> Six different experiments, based on the different particle sizes produced by sieving, were carried out for 4 h and the results are presented in Fig. 1a and b. It is evident that, for particle size classes > 180 μm, diffusion becomes a significant limiting factor even at 800°C, which is considered to be the upper limit for the roasting; consequently, for the subsequent experiments, the raw material was processed down to a size of 200 μm or less.

Once the raw materials were milled and sieved to a size < 200 μm, the particle size distribution of the raw material was measured and a significant quantity of the particles with sizes of less than 200 μm were identified: *D*<sub>(0.5)</sub> = 83.7 μm and *D*<sub>(0.8)</sub> = 161 μm (supplementary Fig. S-2). Following the PSD analysis, a number of additional TGA experiments were performed as a function of temperature, and the collated results are presented in Fig. 1c. It can be clearly seen that, in the initial stages, a number of reactions occur within each sample, as indicated by rapid mass increases; however, the duration of this reactive stage depends on available thermal energy, i.e., temperature. It is known that several different mixed oxides may form during thermal treatment of Nd-Fe-B permanent magnet materials, which leads to phase changes occurring in the magnet materials, as highlighted by Firdaus et al.<sup>7,9</sup> In addition,

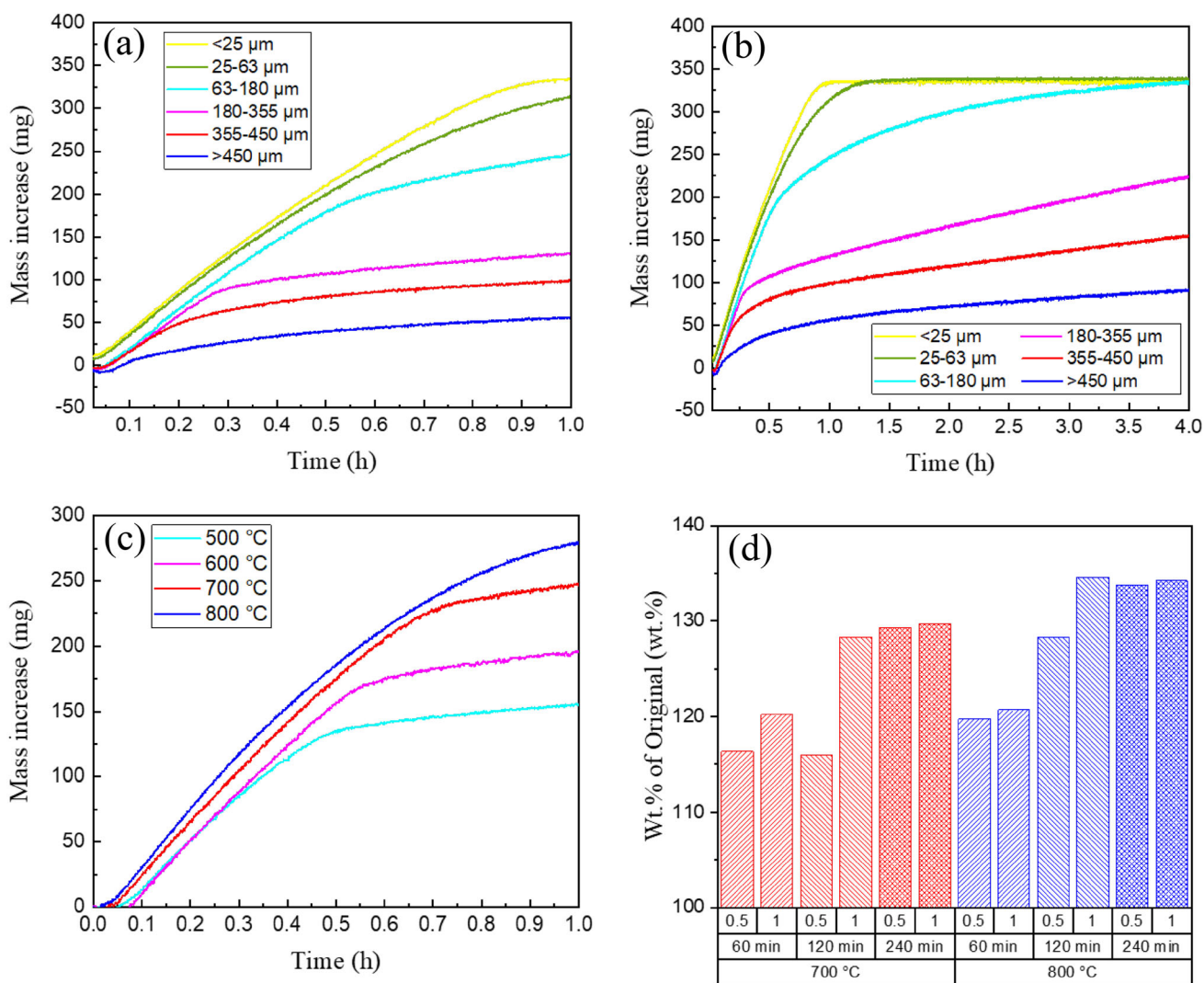


Fig. 1. Influence of (a, b) particle size ( $T = 800^{\circ}\text{C}$ , airflow = 1.0 L/min); (c) temperature (particle size  $< 200\ \mu\text{m}$ , airflow = 1 L/min); (d) airflow (particle size  $< 200\ \mu\text{m}$ ,  $T = 700^{\circ}\text{C}$  and  $800^{\circ}\text{C}$ ,  $t = 30$  and  $60$  min) on the roasting of spent Nd-Fe-B magnet powder.

investigations by Jakobsson et al. show that different possible phases include several oxides and mixed oxides of Fe, Nd and B.<sup>15</sup> The results also demonstrate that the temperature can drastically increase the rate and degree of oxidation, and that temperatures below  $700^{\circ}\text{C}$  are not sufficient to achieve the complete oxidation of the raw materials in the present study. Therefore,  $800^{\circ}\text{C}$  was selected at the temperature for the oxidative roasting of the Nd-Fe-B magnets. XRD results (supplementary Fig. S-3) from samples treated at different temperatures showed that the main phases of the spent magnets after roasting were  $\text{Nd}_2\text{O}_3$  and  $\text{Fe}_2\text{O}_3$ , further indicating that the optimal temperature was  $800^{\circ}\text{C}$ . Conversely, treatment of Nd-Fe-B at an excessive oxidation temperature will result in the formation of Nd-Fe oxide complexes like  $\text{NdFeO}_3$ , which can significantly suppress the leaching of REEs.

Based on the TGA analyses, a horizontal furnace where the flow of technical air could be carefully

controlled was employed for the roasting experiments, and the related results are presented in Fig. 1d. It can be clearly seen that the oxygen partial pressure plays a key role in the roasting process, as highlighted by the noticeable difference between experiments at  $800^{\circ}\text{C}$  with 0.5 L/min and 1 L/min of airflow. In contrast to a rotary kiln where this kind of roasting process would typically be performed, the crucible-based methodology used here requires the diffusion of oxygen through an oxidized layer, which leads to lower oxidation rates and a less efficient process. Moreover, after each of these experiments, it was observed that the particles had become sintered, which is something that would also be prevented by use rotary kiln.

From Fig. 1d, it can be determined that the most suitable conditions for the roasting of spent magnet powder are an airflow of 1 L/min, a temperature of  $800^{\circ}\text{C}$ , and a total roasting time of 2 h. The changes in the content of REEs, Fe and other main elements of interest found in the spent magnet powder before

and after roasting at 800°C are shown in Table I, from which it can be seen, the relative amount of Fe in the material decreased from 62.7% to 46.4% before and after roasting—equal to a net mass gain for the sample of 35%—which indicates that the process successfully oxidizes the Nd-Fe-B powder. The post-roast analysis of Nd, Pr, Dy, Gd and Ho also highlights the significant differences in total elemental content of these REEs (25.8%) when compared to B and Co (both > 0.6%). It should also be noted that, due to the exothermic nature of the oxidation process, the temperature in the preheated sample was found to increase above the set temperature by ca. 30°C.

### Leaching of Roasted Magnet Wastes

Following the roasting of Nd-Fe-B powder in a horizontal furnace, the roasted powder was subject to acid leaching in order to determine whether the material was sufficiently oxidized, so that the complete dissolution of iron and the related effects of leached ferrous ions on final product purity as well as hydrogen gas formation could be avoided. Two of the most commonly used leaching systems, based on sulfuric and hydrochloric acid leaching, were selected for the recovery of REEs, Co, B and Fe from roasted Nd-Fe-B material for investigation, and the results were compared.

#### Sulfuric Acid Leaching

The effect of sulfuric acid concentration (0.5–4 mol/L) on the leaching of REEs, Fe, Co and B from roasted demagnetized sample was investigated at 80°C with an  $L/S = 10$ , and the results are displayed in Fig. 2a, b, c, and d. It was found that the leaching of REEs (Fig. 2a) increased with increasing sulfuric acid concentration until a maximum extraction rate of 99.4% was reached at 3 mol/L. Further increase in the sulfuric acid concentration to 4 mol/L was observed to cause a decrease in the REEs leaching efficiency, due to the decrease in the solubility of REE sulfates with the increase of sulfate ion concentrations.<sup>16,17</sup> This was confirmed by XRD results of the leach residues, which found the presence of REE sulfates at the highest sulfuric acid concentration (supplementary Fig. S-4).

Figure 2a highlights how an increase in sulfuric acid concentration can enhance the leaching kinetics of REEs, as shown by the decrease in optimum leaching time from 180 min to 60 min as the sulfuric acid concentration is changed from

0.5 mol/L to 3 mol/L. In contrast, Fig. 2b clearly illustrates that, after roasting, Fe leaching kinetics are much slower than either REEs, B or Co. Although the leaching is seen to increase somewhat with higher sulfuric acid concentrations and prolonged reaction times, the maximum leaching of iron attained was only ~ 50% after 240 min with 4 mol/L. Moreover, at the lowest  $H_2SO_4$  concentration (0.5 mol/L), the dissolution of iron was found to increase for the first 60 min of leaching time, before steadily decreasing for the remainder of the experiment to ca. 12% after 240 min. The main reason for this observation is that the dissolved Fe can be hydrolyzed to form an  $Fe(OH)_3$  precipitate, due to sulfuric acid consumption, and ends up in the leach residue. These results highlight the possibility that low acid concentrations can achieve the selective separation of REEs and Fe during leaching.

When compared with the leaching behaviors of REEs and Fe, the leaching of boron with 0.5 mol/L  $H_2SO_4$  can achieve levels of > 85% within 60 min (Fig. 2c). Further increases in sulfuric acid concentration to 4 mol/L results in over 95% of B being leached within 40 min; however, the findings show that prolongation of leaching time beyond 60 min results in only a modest enhancement. Cobalt, on the other hand, is unable to be effectively leached under low acid conditions, with only 50% of Co found in solution after 240 min with 0.5 mol/L  $H_2SO_4$  (Fig. 2d), and this may be due to the low solubility of  $CoFe_2O_4$  or  $Co_3O_4$  formed during roasting at 800°C.<sup>18–20</sup> Nevertheless, the level of Co leaching was seen to improve from 50% to 95% when the sulfuric acid concentration increased from 0.5 mol/L to 4 mol/L.

#### Hydrochloric Acid Leaching

In order to compare the different behaviors of the investigated metals between the hydrochloric and sulfuric acid leaching systems, the effects of HCl concentration (0.5–4 mol/L) on Nd-Fe-B leaching were examined under equivalent experimental conditions ( $L/S = 10$ ,  $T = 80^\circ C$ ). The results for REEs, Fe, Co and B leaching with HCl are shown in Fig. 3a, b, c, and d).

Figure 3a, c, and d all show that the respective leaching equilibrium times of REEs, B and Co all reduce as the hydrochloric acid concentration is increased from 0.5 mol/L to 4 mol/L; for example, > 99% REEs are leached within 40 min using 4 mol/L HCl. Furthermore, it was also found that

**Table I. Chemical composition of spent Nd-Fe-B magnet powder before and after roasting**

Elements	Fe	Nd	Pr	Dy	Gd	Ho	B	Co
Before (wt.%)	62.7	25.8	6.1	1.8	0.19	0.84	0.96	0.87
After (wt.%)	46.4	19.2	4.6	1.3	0.14	0.62	0.71	0.64

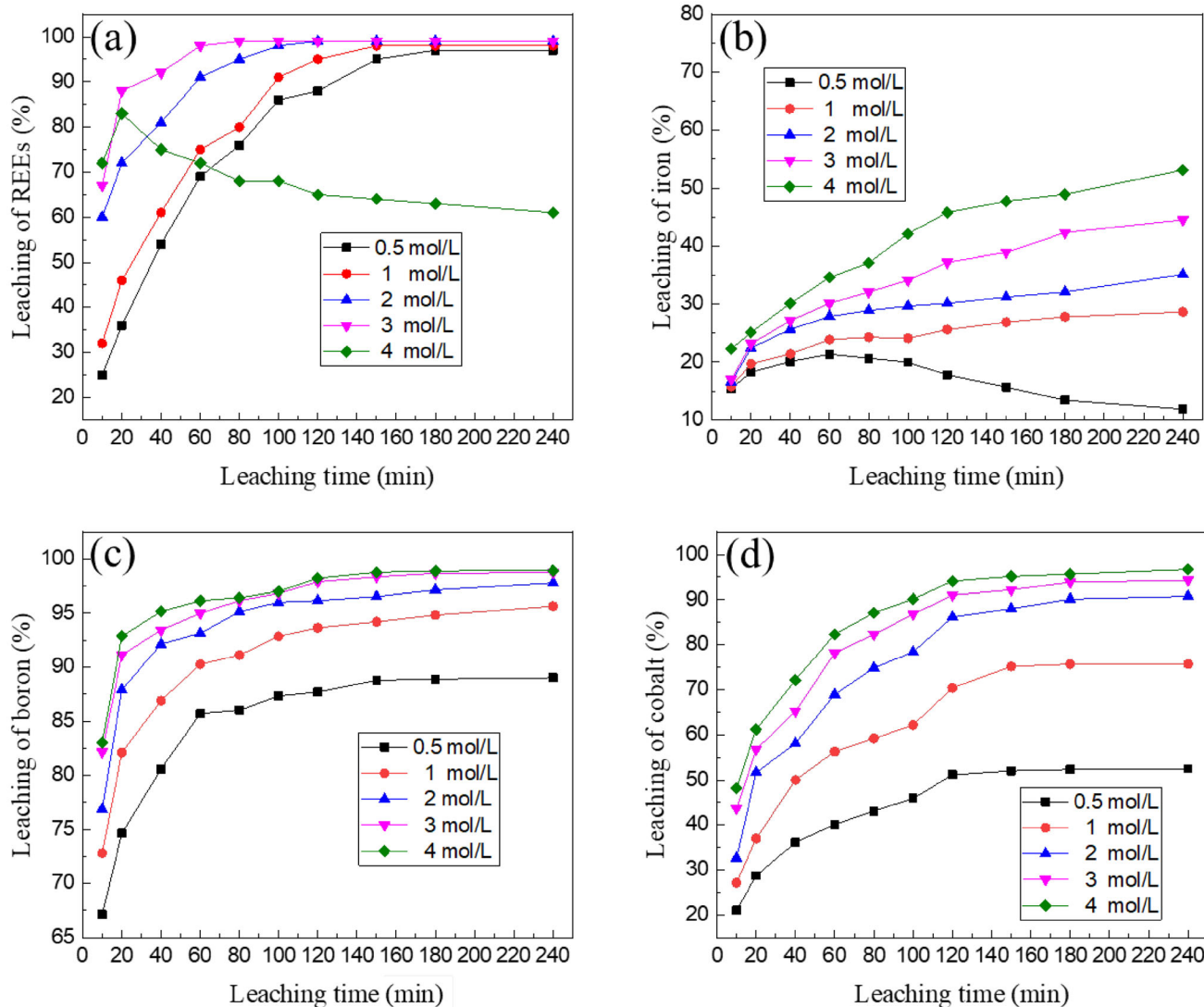


Fig. 2. Kinetics of (a) REEs, (b) Fe, (c) B and (d) Co leaching from roasted Nd-Fe-B powder in different sulfuric acid solution concentrations ( $T = 80^{\circ}\text{C}$ ,  $L/S = 10$ ).

1 mol/L HCl is sufficient to achieve almost complete REEs leaching after only 100 min so that, when compared to sulfuric acid leaching, demonstrates the leaching of REEs with hydrochloric acid solution is more facile. Figure 3c highlights that a similar behavior is also found for boron, which shows higher levels of leaching with 0.5 mol/L HCl after 60 min than the equivalent concentration of H<sub>2</sub>SO<sub>4</sub> (> 95% cf. 85%; Fig. 2c). Further increases in the HCl concentration were also found to enhance the leaching kinetics of B to a level of 99% within 20 min at 4 mol/L HCl.

As was the case with the sulfuric acid solution, leaching of cobalt with hydrochloric acid is more difficult than boron and REEs in low acid concentrations due to the presence of CoFe<sub>2</sub>O<sub>4</sub> or Co<sub>3</sub>O<sub>4</sub> formed during roasting.<sup>19,20</sup> For example, Co leaching only reached 20% after 240 min with 0.5 mol/L HCl (Fig. 3d); however, when the results from

1 mol/L HCl are compared to sulfuric acid with the equivalent H<sup>+</sup> ion concentration (0.5 mol/L H<sub>2</sub>SO<sub>4</sub>; Fig. 2d), the leaching of cobalt with hydrochloric acid is almost 20% greater due to a redox reduction reaction between the cobalt oxides and chloride ions.<sup>21</sup> On the other hand, the leaching of iron was found to increase substantially when the initial HCl concentration was > 1 mol/L, with nearly 45% Fe leached within 240 min for 4 mol/L HCl (Fig. 3b). Nonetheless, as was also observed for sulfuric acid, at the lowest HCl acid concentration (0.5 mol/L) investigated the leaching of iron decreases gradually after 60 min, due primarily to the hydrolysis of iron at pH > 2, such that only 1% of iron is leached after 240 min.

### REEs Recovery from Leachate

After processing of roasted spent magnets in HCl or H<sub>2</sub>SO<sub>4</sub> media, the conventional

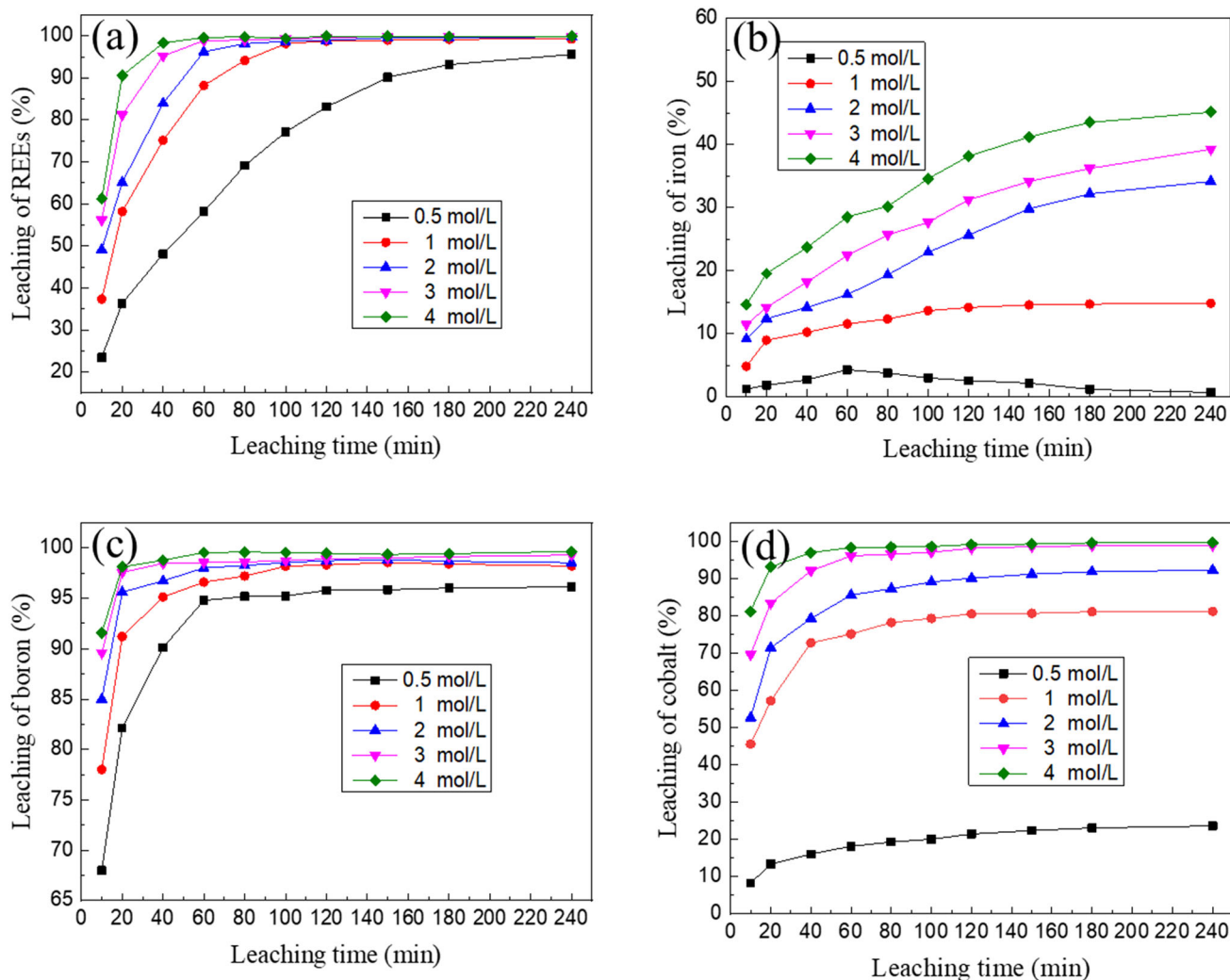


Fig. 3. Kinetics of (a) REEs, (b) Fe, (c) B and (d) Co leaching from roasted Nd-Fe-B powder in different hydrochloric acid solution concentrations ( $T = 80^{\circ}\text{C}$ ,  $L/S = 10$ ).

hydrometallurgical process for the recovery of REEs mainly include: (1) double-sulfate salts ( $\text{NaREE}(\text{SO}_4)_2 \cdot n\text{H}_2\text{O}$ ) precipitation, and (2) REE oxalates ( $\text{REE}_2(\text{C}_2\text{O}_4)_3 \cdot n\text{H}_2\text{O}$ ) precipitation. Typically, double-sulfate precipitation methods are used to recover the REEs in sulfuric acid leach solution due to the large amounts of sulfate ions present, whereas oxalic acid is preferable for the recovery of REEs from hydrochloric acid solution, as a very high excess of sodium and sulfate ions are not required.

When the recovery of REEs and the subsequent leachate purification and separation steps are taken into account, initial acid concentrations of 1 mol/L for both HCl and  $\text{H}_2\text{SO}_4$  were selected as being optimal. In addition to the results, the most suitable leaching time for sulfuric acid leaching and hydrochloric acid leaching were determined to be 150 min and 100 min, respectively. The main

composition of the leachates achieved based on these parameters are shown in Table II.

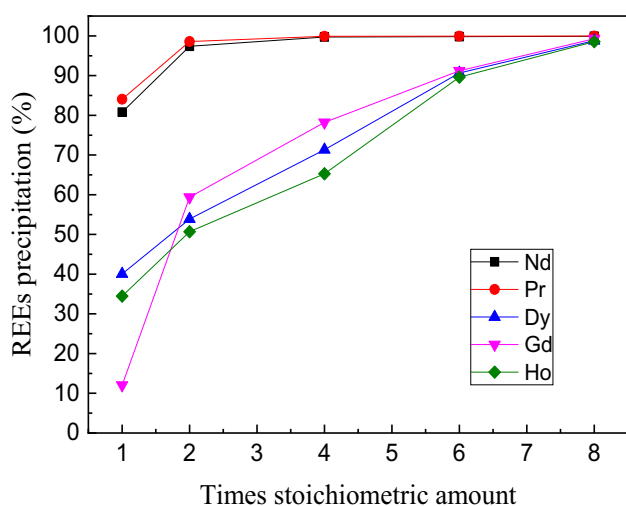
#### *REEs Recovery Using Double Salt Precipitation for PLS1*

The effect of sodium sulfate concentration was studied by varying the amount of  $\text{Na}_2\text{SO}_4$  added to the PLS1 solution between 1 and 8 times the stoichiometric quantity required, as indicated by Eq. 1. All the experiments were performed at a temperature of  $70^{\circ}\text{C}$  for 60 min, and the results are shown in Fig. 4. As can be seen, under these experimental conditions, the light RREs (Pr and Nd) were found to precipitate more readily than the heavy RREs (Gd, Dy and Ho).

In terms of Nd and Pr, it was found that approximately 99% could be recovered when a  $\text{Na}_2\text{SO}_4$  stoichiometric ratio of 2 was utilized, and

**Table II. Composition of the sulfuric acid leachate (PLS1) and hydrochloric acid leachate (PLS2)**

No.	Concentration (g/L)								
	Fe	Co	B	Nd	Pr	Gd	Dy	Ho	REEs
PLS1	12.3	0.48	0.67	19.1	4.5	0.14	1.3	0.60	25.7
PLS2	6.3	0.50	0.69	19.0	4.4	0.13	1.3	0.61	25.5

Fig. 4. Effect of  $\text{Na}_2\text{SO}_4$  additions on the precipitation of REEs concentrations ( $T = 70^\circ\text{C}$ ,  $t = 60$  min).

that only very minor increases occurred with further  $\text{Na}_2\text{SO}_4$  additions. In contrast, with the same amount of sodium sulfate, the precipitation efficiencies for Gd, Dy and Ho all were less than 60%, due to the fact that heavy REE double-sulfate salts exhibit higher solubility when compared with the equivalent light and medium REE double-sulfate salts.<sup>11</sup> A recovery level of  $> 98\%$  for the heavy REEs could be achieved with a stoichiometric ratio of 8 ( $\text{Na}_2\text{SO}_4$  to REEs); however, overall, the total amount of REEs recovered only increased from 97.4% to 99.4%. Consequently, with these solutions, high levels of sodium sulfate should only be added if the recovery of heavy REEs like Gd, Dy and Ho is desired or the level of REEs needs to be reduced due to environmental concerns. Solution concentrations of Pr, Nd, Gd, Dy and Ho decreased to a level of  $< 50$  mg/L measured after precipitation with 8 times the stoichiometric amount of  $\text{Na}_2\text{SO}_4$ . XRD (supplementary Fig. S-5a) and SEM (supplementary Fig. S-6a-b) analysis of the main phases present within the precipitate shows that structures comprise  $\text{NaRE}(\text{SO}_4)_2 \cdot n\text{H}_2\text{O}$  with a hexagonal crystal configuration. After the double-sulfate precipitation, the REE products obtained were converted to their respective hydroxides,  $\text{REE}(\text{OH})_3$ , by treatment with a 1.1 times the stoichiometric amount of NaOH at  $70^\circ\text{C}$  (supplementary Fig. S-5b). The resultant particles of the mixed REE hydroxides were found to have a

tetrahedron configuration and a size ranging from  $1 \mu\text{m}$  to  $2 \mu\text{m}$  (supplementary Fig. S-6c-d). The main metal content in the REEs double-sulfate salts and REE hydroxides were determined by chemical analysis, and the results showed that impurities like Co and Fe are less than 0.01%, which demonstrates that the double-salt precipitation method can produce high-purity REE materials (Table III). In addition, the obtained sodium sulfate products after REE hydroxide conversion can be reused again for REEs precipitation from sulfuric acid leachate.<sup>22</sup>

#### REEs Recovery Using Oxalate Precipitation for PLS2

The solution obtained after hydrochloric acid leaching (PLS2) was treated by the oxalate precipitation process to recover the REEs, and the effect of oxalic acid additions at  $50^\circ\text{C}$  with 60-min reaction time on the rate of precipitation and purity of the final products was investigated. Figure 5a shows that the precipitation of REEs increased significantly as the level of oxalic acid in the system increased. The precipitation of Nd, Pr, Dy, Gd and Ho all reached ca. 99% with only 1.8 times the stoichiometric amount of oxalic acid. At the same time, however, the Fe and Co content increased to 1.28% and 0.24%, respectively, leading to a reduction in the final product purity (Fig. 5b). Subsequent XRD analysis (supplementary Fig. S-7a) showed that the main phases found in the products were hydrated REE oxalates,  $\text{REE}_2(\text{C}_2\text{O}_4)_3 \cdot n\text{H}_2\text{O}$ , which had an excellent crystallinity and a particle size within the range of  $1\text{--}5 \mu\text{m}$  (supplementary Fig. S-8a-b). The REE oxalates obtained were further treated by roasting at  $800^\circ\text{C}$  for 120 min in order to produce mixed oxides of Nd, Pr, Dy, Gd and Ho, as confirmed by subsequent XRD analysis (supplementary Fig. S-7b). These yellow-green REE oxides were found to be rectangular in shape and have a size range of  $2\text{--}5 \mu\text{m}$  (supplementary Fig. S-8c-d).

It has been previously reported that the presence of Fe(II) in oxalate solutions can have a negative impact on the purity of the final REE products.<sup>23</sup> From chemical analysis, it was determined that approximately 40% of the iron dissolved in the hydrochloric acid leach solution was in the form of Fe(II); therefore, in order to produce high-purity REEs products from HCl-based leaching, the



**Table III. Chemical composition of double-sulfate salt and REE hydroxides (wt.%)**

Elements	REEs	Co	B	Na	Fe	SO <sub>4</sub> <sup>2-</sup>
NaRE(SO <sub>4</sub> ) <sub>2</sub> ·nH <sub>2</sub> O	38.05	< 0.01	< 0.01	6.82	< 0.01	51.21
RE(OH) <sub>3</sub>	73.25	< 0.01	< 0.01	0.14	< 0.01	0.86

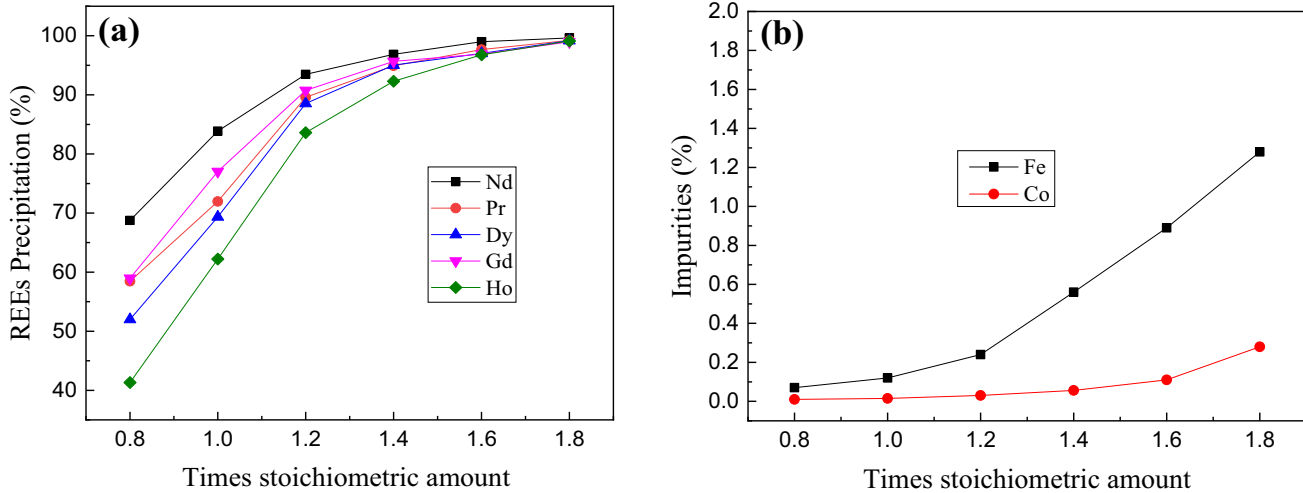


Fig. 5. (a) The effect of oxalic acid amounts on the REEs precipitation and (b) the related of Fe and Co content in the resultant REEs-oxalate products ( $T = 50^{\circ}\text{C}$ ,  $t = 60 \text{ min}$ ).

oxidation of Fe(II) is required. The drawback, however, is that the presence of ferric ions, rather than ferrous, will result in a substantial increase in oxalic acid consumption due to the strong complexation that occurs between the oxalate anions with the ferric cations. Consequently, the ability to produce a low-cost and high-purity REE product with oxalate precipitation from a solution with a relatively high concentration of iron is currently not achievable with this technique. Furthermore, effective methods for the recovery of oxalic acid from high ferric ion waste solutions that result from this type of procedure also remain a challenge.

## CONCLUSION

1. During the roasting process, both the particle size and temperature have a significant effect on the product composition. An insufficient level of roasting results in poor selectivity due to enhanced levels of Fe<sup>2+</sup> dissolution, so 800°C was selected as suitable roasting temperature.
2. Increasing acidity in sulfuric and hydrochloric solution media can both improve the leaching kinetics of REEs, Co, Fe and B from Nd-Fe-B materials. Nevertheless, with sulfuric acid leaching, REE solution enrichment to high concentrations is not possible due to the relatively low solubility of REE sulfates. In contrast, the leaching of REEs, boron and cobalt were all found to be more facile in hydrochloric acid

solution. Generally, in both H<sub>2</sub>SO<sub>4</sub> and HCl leaching systems, low acid concentrations were more conducive to selective separation of REEs over Fe.

3. For REE-enriched sulfate solutions, the double-sulfate precipitation method can achieve an effective separation of REEs, and their subsequent recovery is less affected by the presence of impurities like iron and cobalt. However, in order to achieve the total separation of all REEs, in particular the so-called heavy REEs, > 8 times stoichiometric amount of Na<sub>2</sub>SO<sub>4</sub> additive is required. In the case of REEs in hydrochloric acid solution, the presence of ferrous and cobalt ions have a relatively adverse effect on the purity of the final products and the oxidation of Fe(II) to ferric ion Fe(III), resulting in a higher consumption [ $n(\text{oxalic acid})/n(\text{REEs}) > 3$ ] of oxalic acid during the precipitation process.
4. After REE double-sulfate precipitation, the circulation of sodium sulfate can reduce the production cost for REEs recovery in sulfuric acid solution. For oxalate precipitation, the oxalic acid recovery from high ferric solutions is a challenge because the strong complexing ability of iron and oxalic acid. Moreover, the oxalate ions are unable to be recovered after calcination. In addition, regardless of the leaching system, the treatment of boron-containing wastewater is a necessity for sustainable recycling of permanent magnets.

## ACKNOWLEDGEMENTS

Open access funding provided by Aalto University. The authors acknowledge HYMAG project (SL/84/04.03.00.0400/2017) funded by the Regional Council of Satakunta, AIKO funding. This paper also made use of the Academy of Finland's Raw-MatTERS Finland Infrastructure (RAMI) based at Aalto University and the Association of Finnish Steel and Metal Producers (METSEK-project). The authors would also like to acknowledge the financial support from the National Nature Science Foundation of China (No.51804141) as well as the Science and Technology Project of the Education Department of Jiangxi Province (GJJ170533).

## OPEN ACCESS

This article is distributed under the terms of the Creative Commons Attribution 4.0 International License (<http://creativecommons.org/licenses/by/4.0/>), which permits unrestricted use, distribution, and reproduction in any medium, provided you give appropriate credit to the original author(s) and the source, provide a link to the Creative Commons license, and indicate if changes were made.

## ELECTRONIC SUPPLEMENTARY MATERIAL

The online version of this article (<https://doi.org/10.1007/s11837-019-03844-7>) contains supplementary material, which is available to authorized users.

## REFERENCES

- R. Schulze and M. Buchert, *Resour. Conserv. Recycl.* 113, 12 (2016).
- European Commission, "Communication From The Commission To The European Parliament, The Council, The European Economic And Social Committee And The Committee Of The Regions on the 2017 list of Critical Raw Materials for the EU", <http://eur-lex.europa.eu/legal-content/EN/ALL/?uri=COM:2017:0490:FIN>. Accessed 18 July 2019.
- M.K. Jha, A. Kumari, R. Panda, J. Rajesh Kumar, K. Yoo, and J.Y. Lee, *Hydrometallurgy* 165, 2 (2016).
- W.H. Wells Jr and V.L. Wells, Chapter 21: the lanthanides, rare earth elements, in *Patty's Toxicology*, 6th edn. ed. by E. Bingham and B. Cofrissen (Amsterdam: Wiley, 2012), pp. 817–840.
- M.A. Reuter, C. Hudson, A. Van Schaik, K. Heiskanen, C. Meskers, and C. Hagelüken, *Metal Recycling: Opportunities, Limits, Infrastructure, A Report of the Working Group on the Global Metal Flows to the International Resource Panel* (UNEP, 2013).
- Y. Yang, A. Walton, R. Sheridan, K. Guth, R. Gauß, O. Gutfleisch, M. Buchert, B. Steenari, T. Van Gerven, P.T. Jones, and K. Binnemans, *J. Sustain. Metall.* 3, 122 (2017).
- M. Firdaus, M.A. Rhamdhani, W.J. Rankin, M. Pownceby, N.A.S. Webster, A.M. D'Angelo, and K. McGregor, *Corros. Sci.* 133, 374 (2018).
- T. Vander Hoogerstraete and K. Binnemans, *Green Chem.* 16, 1594 (2014).
- M. Firdaus, M.A. Rhamdhani, Y. Durandet, W.J. Rankin, and K. McGregor, *Corros. Sci.* 133, 318 (2018).
- M. Tanaka, T. Oki, K. Koyama, H. Narita, and T. Oishi, Chapter 255—Recycling of rare earths from scrap, in *Handbook on the Physics and Chemistry of Rare Earths*, Vol. 43 (2013), pp. 159–211.
- G. Das, M.M. Lencka, A. Eslamimanesh, P. Wang, A. Anderko, R.E. Riman, and A. Navrotsky, *J. Chem. Thermodyn.* 131, 49 (2019).
- D. Chung, E. Kim, E. Lee, and J. Yoo, *J. Ind. Eng. Chem.* 4, 277 (1998).
- D. Panias, M. Taxiarchou, I. Paspaliaris, and A. Kontopoulos, *Hydrometallurgy* 42, 257 (1996).
- P. Halli, P. Taskinen, and R.H. Eric, *J. Sustain. Metall.* 3, 191 (2017).
- L.K. Jakobsson, G. Tranell, and I. Jung, *Metall. Trans. B* 48, 60 (2017).
- H. Yoon, C. Kim, K.W. Chung, S. Lee, A. Joe, Y. Shin, S. Lee, S. Yoo, and J. Kim, *Korean J. Chem. Eng.* 31, 706 (2014).
- D. Beltrami, J.D. Gauthier, S. Bélair, and V. Weigel, *Hydrometallurgy* 157, 356 (2015).
- R.C. Hubli, J. Mitra, and A.K. Suri, *Hydrometallurgy* 44, 125 (1997).
- C. Tang, C. Wang, and S. Chien, *Thermochim. Acta* 473, 68 (2008).
- N.R.E. Radwan and H.G. El-Shobaky, *Thermochim. Acta* 360, 147 (2000).
- Z. Takacova, T. Havlik, F. Kukurugya, and D. Orac, *Hydrometallurgy* 163, 7 (2016).
- A. Porvali, V. Agarwal, and M. Lundström, *Min. Metall. Explor.* (2019). <https://doi.org/10.1007/s42461-019-0086-2>.
- P. Venkatesan, Z.H.I. Sun, J. Sietsma, and Y. Yang, *Sep. Purif. Technol.* 191, 384 (2018).

**Publisher's Note** Springer Nature remains neutral with regard to jurisdictional claims in published maps and institutional affiliations.